Eur. Phys. J. A (2023) 59:94
https://doi.org/10.1140/epja/s10050-023-01006-7

THE EUROPEAN PHYSICAL JOURNAL A

Review

Perspective on superconducting qubit quantum computing

Olivier Ezratty[a]

EPITA, Paris, France

Received: 12 March 2023 / Accepted: 12 April 2023 / Published online: 2 May 2023

Communicated by Denis Lacroix

Abstract This perspective describes the history, scientific and technology developments of superconducting qubit-based quantum computers, which are currently dominant, particularly with industry vendors. Adopting an engineering viewpoint, it showcases the great diversity of technology options, explains how superconducting qubit chipsets are manufactured, describes some challenges with how qubits are driven by classical electronics, how to improve their fidelities and how their energetic footprint can be optimized. We also briefly describe the current status of so-called NISQ (noisy intermediate scale quantum) computers and the resource estimations to run their potential use cases, particularly for running quantum many-body physics simulations.

1 Introduction

Superconducting qubits are currently the leading technology in the quantum computing commercial space, being exploited or chosen by IBM, Google, Rigetti, Amazon, Alibaba, Baidu as well as many startups such as IQM (Finland), OQC (UK), Anyon Systems (Canada), Alice&Bob (France), Nord Quantique (Canada) and others. It is the currently best scalable architecture in the gate-based model, with a record of 433 qubits with IBM and 121 qubits in China as of January 2023 [1,2], although, so far, the quality of these qubits is still insufficient for these being useful on a practical basis.

The Josephson junction used in these qubits is a thin nanometric insulating barrier between two superconducting metals, creating a tunnel junction. It creates a quantum electrical component with a single degree of freedom, the superconducting phase difference between its electrodes, conjugated to the number of Cooper pairs passed through the junction. The supercurrent through the junction (direct current Josephson effect) is driven by the phase difference. From the electrical point of view, a Josephson junction behaves as a non dissipative and non-linear inductance whose value depends on the phase, and thus on the current. Superconducting qubits have the particularity of being the only mainstream ones that are macroscopic, in the sense that they are not linked to the control of a single particles such as individual atoms, electrons or photons, as in most other qubit technologies.

At superconducting temperature well below the superconductivity critical temperature, Josephson junctions embedded in an electrical circuit behave as an artificial atom, with gate and/or flux controlled quantum levels and about 10^{11} electrons (100 billion) of electron Cooper pairs.

They form an artificial atom with precisely controllable energy levels according to their parameters comprising a Josephson barrier, some capacitances and inductances connected in series and/or in parallel and some readout circuits using a nearby resonator. This artificial atom property was first demonstrated in 1985 [3].

Superconducting qubits use non dissipative elements: capacitors, inductors and the Josephson junction which act as a nonlinear non-dissipative inductor. Capacitors store energy in the electric field while inductors store energy in the magnetic field. But at any non-zero frequency, superconductors still dissipate some power, through two channels: the transport by the Cooper pairs and by normal charge carriers (quasi-particles), that is proportional to the quasi-particle density, which diminishes exponentially at low temperatures.

In this paper that is based on the open sourced book "Understanding Quantum Technologies 2022", we assume the reader is already familiar with what is a gate-based quantum computer, how qubits operate from a mathematical standpoint and have some knowledge of quantum physics and classical electronics engineering [4].

Olivier Ezratty is a cofounder of the Quantum Energy Initiative.

Topical Issue—Quantum Computing in Low-Energy Nuclear Theory.

[a] e-mail: olivier@oezratty.net (corresponding author)

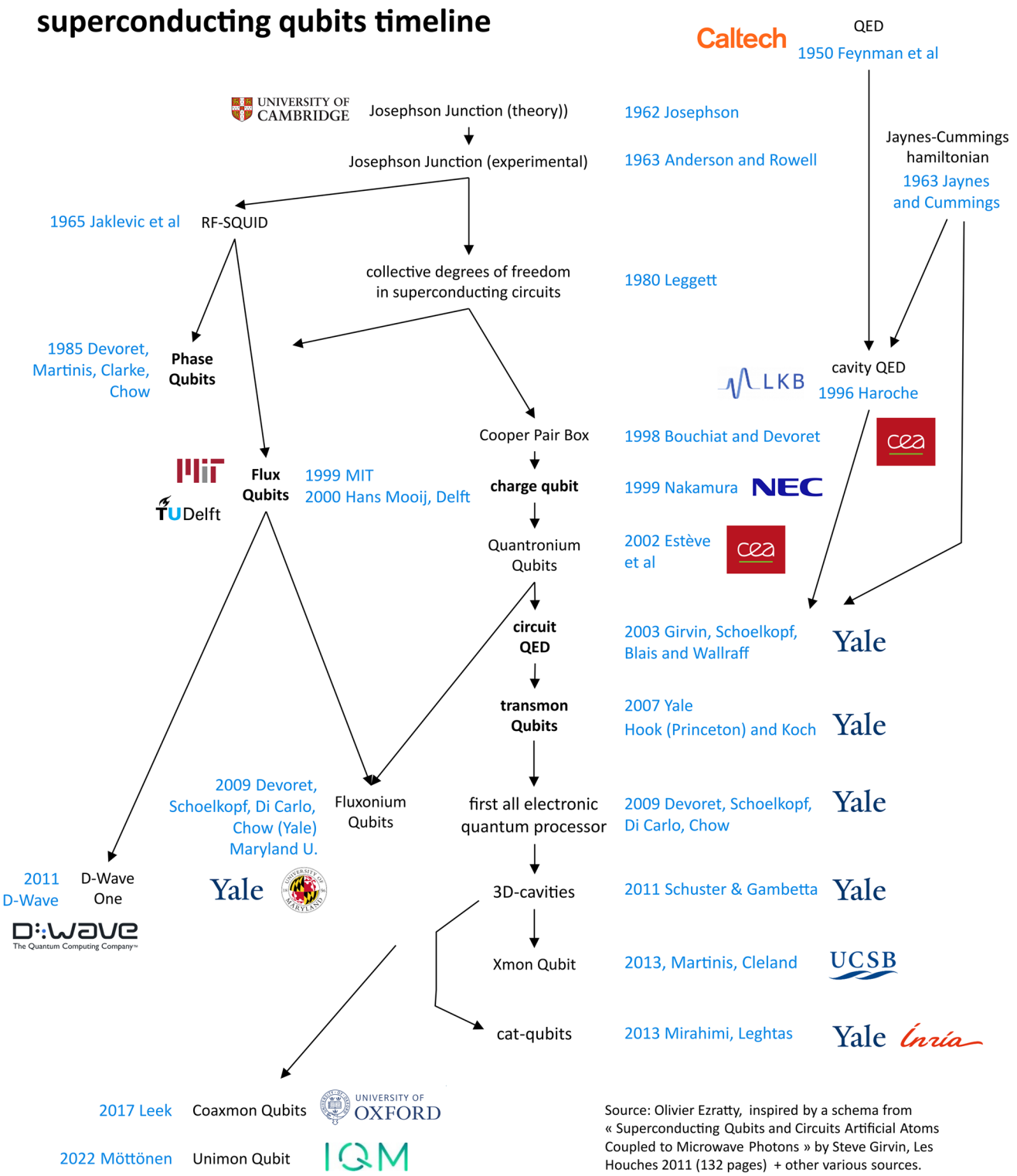

Fig. 1 A historical timeline of superconducting qubits. The contribution of scientists at Yale University seems dominant here, thus the nickname of the "Yale gang". (cc) Ezratty [4]

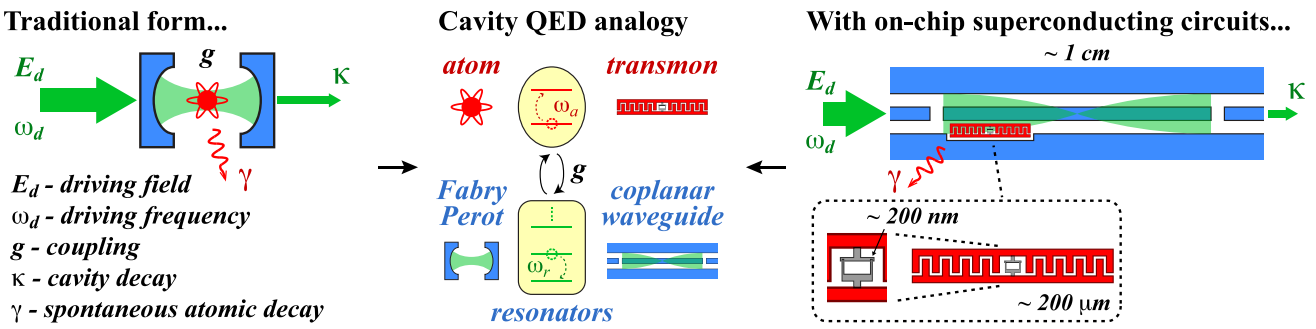

Fig. 2 Principles of circuit QED starting with cavity QED describing the interactions between neutral atoms and photons in cavities to their derivation as circuit QED in superconducting qubits. Source: Langford [17]

2 A bit of history

The history of superconducting qubits started in the mid-1980s but you need to fly back to 1957 with the elaboration of the BCS theory that explained (partially) how pairs of opposite spin electrons—*aka* Cooper pairs—behave at low temperatures, generating the superconducting effect. Then, 1962 marks the Josephson effect discovery by Brian Josephson, completed by its experimental proof in 1963 by John M. Rowell from the Bell Labs [5].

In 1980, Antony Leggett modelized the collective degrees of freedom of superconducting circuits. A bit like a Bose-Einstein condensate of cold neutral atoms, Cooper-pairs of electrons in a superconducting material behave like a single quantum object with its own quantum wave. Antony Leggett understood that the quantum behavior of a Josephson junction, if any, can be inferred from its classical behavior.

In 1985, John Clarke, Michel Devoret (his post-doc) and John Martinis (his PhD student), demonstrated the phenomenon of Macroscopic Quantum Tunneling of a current-biased Josephson junction out of its zero-voltage state. Soon after, they demonstrated quantum levels for the phase. This was the first artificial electrical atom [3].

Back then, the JJ (the little nickname for Josephson junctions) was implemented with Nb–NbO_x–PbIn (niobium, lead, indium) and cooled with a He_4-based cryostat.

In 1998, Vincent Bouchiat, then a PhD in Michel Devoret, Daniel Esteve and Cristian Urbina's Quantronics group at CEA-Saclay in France, implemented the first Cooper Pairs Box (CPB) and characterized its ground state. Pratically speaking, a Cooper pair box is a JJ connected to a voltage source by a capacitor on one side, and a Josephson junction on the other side.

The first demonstration of quantum coherent superposition with the first excited state was achieved in 1999 by Yasunobu Nakamura with Yuri Pashkin and Jaw-Shen Tsai at NEC Labs in Tsukuba, Japan [6].

It was the first "charge qubit" per se, with a tiny coherence time of 2 ns. They extended it in 2001, implementing the first measurement of Rabi oscillations associated with the transition between two Josephson levels in the Cooper pair box, using the configuration developed by Vincent Bouchiat and Michel Devoret in 1998. A first functional qubit version of the Cooper pair box, the quantronium, was demonstrated by the CEA-Saclay Quantronics team in 2002. More technical insights of what was achieved in Japan and France between 1999 and 2022 can be found in [7]. It took about 12 years to CEA's team to reach four qubits as described in [8].

The modern version of the CPB circuit, the transmon, was developed at Yale University in 2006. The Yale University research teams led by Rob Schoelkopf, Michel Devoret and Steve Girvin welcomed many talented theoreticians and experimentalists who were key contributors to the progress of transmon qubits as shown in the timeline in Fig. 1. Alexandre Blais and Andreas Wallraff developed around 2003–2004 the key principles of circuit QED (cQED) as shown in Fig. 2 [9–12].

It allowed quantum non-demolition readout of qubit state in the dispersive regime. A QND readout happens after measurement collapses the wave function onto $|0\rangle$ or $|1\rangle$ and a subsequent readout will yield the same $|0\rangle$ or $|1\rangle$. Then, David Schuster and Jay Gambetta created between 2007 and 2011 2D and 3D cavity resonators designs [13–15]. Jens Koch created Cooper pair boxes with a large shunting capacitance which created a modest reduction in anharmonicity and enabled strong coupling with microwave photons [16].

Jerry Chow was also a key contributor between 2005 and 2010 and has since then been at IBM, now leading their quantum hardware system developments in Jay Gambetta's team. In 2009. Devoret, Schoelkopf, Leonardo Di Carlo (now at TU Delft), Jerry Chow et al. created the first programmable two-qubit processor and implemented a small Grover search on it. The first functional two-qubit processor fully fitted with a universal set of gates and individual single-shot qubit readout was then in 2012 demonstrated with Grover's search algorithm by A. Dewes et al. at CEA Saclay [18].

Blake Robert Johnson proposed in 2011 to use a Purcell filter to protect a qubit from spontaneous emission coming

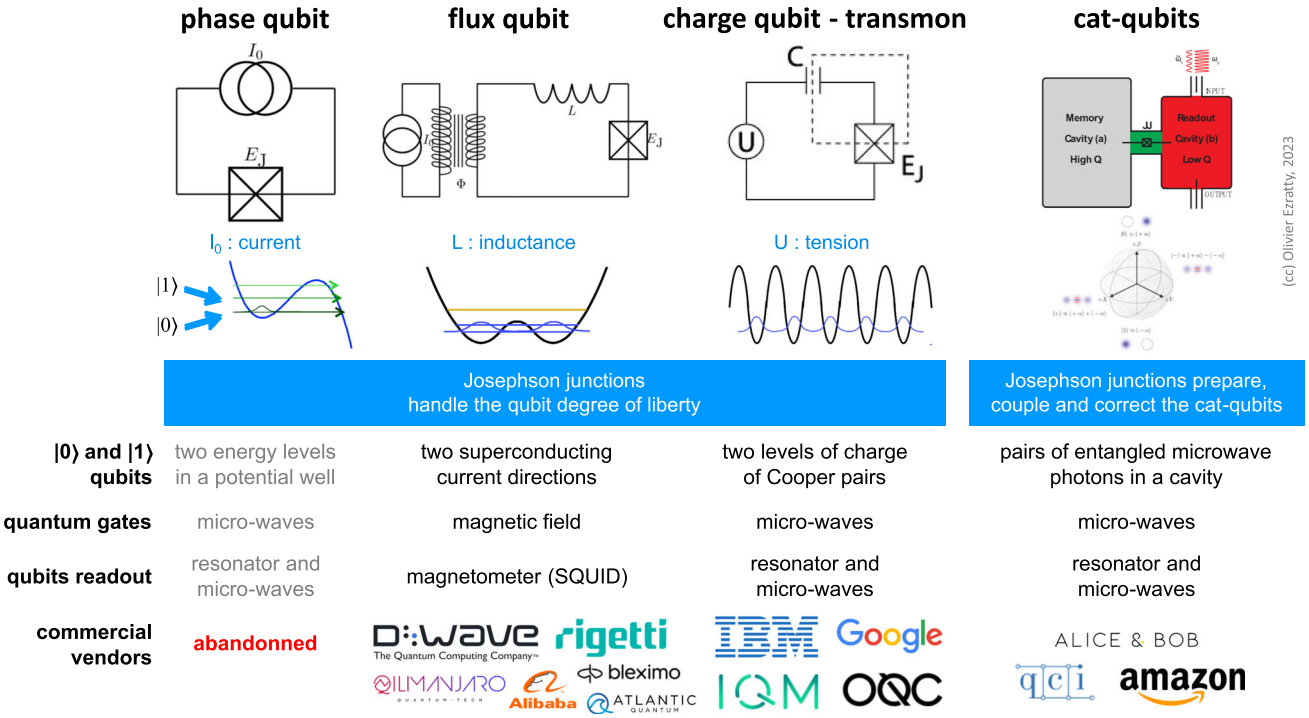

Fig. 3 The different types of superconducting qubits and the related industry vendors. inspired from [41] and [42] with additions from Ezratty

from the Purcell effect that is a relaxation through the readout resonator. It's a mix of low-pass and high-pass microwave filter [19–21]. The spontaneous emission rate (SER) is one key contributor that affects a superconducting qubit coherence time T_1.

In another domain, Matt Reagor and Hanhee Paik improved in 2013 the stability of microwaves and qubit coherence (T_1/T_2) with transmons embedded in 3D cavities [22].

Other contributions worth mentioning are Hans Mooij (TU Delft) who created a flux-qubit with three Josephson junctions in 1999 with experiments done in 2000. Andrew Hook (Princeton) contributed to the development of the transmon qubit. In 2010, Andrew Cleland, John Martinis and their PhD Arron O'Connell were able to entangle three flux superconducting qubits and to control it with a mechanical resonator [23]. It led to the creation of the Xmon tunable qubit in 2013 [24] which was later used by Martinis at Google after 2014. Andrew Cleland now runs his own lab at the University of Chicago.

In 2017, Peter Leek then at Oxford created the coaxmon superconducting qubit, where the qubit and resonator are on opposing sides of a single chip, with control and readout wiring being provided by coaxial wiring running perpendicular to the chip plane [25]. It led the same year to the creation of OQC. In 2022, Mikko Möttönen from IQM created the Unimon superconducting qubit with a simpler setting, better nonlinearity and fidelities [26]. However, both these qubits have not yet showcased improved figures of merit vs the state of the art.

Then, cat-qubits were created in 2013 by Mazyar Mirrahimi at Yale with Michel Devoret, with later contributions by Zaki Leghtas and many advances since then.

Let's now circle back to the different types of superconducting qubits that differ in the way they encode quantum information in two distinct states (see Fig. 3).

Phase Qubits use larger Josephson junctions than in charge qubits. Their state corresponds to two levels of current energy in a Josephson junction. This approach was tested by NIST in the USA among other places but no commercial vendor seems to use this type of superconducting qubit. John Martinis tested such qubits back in 2012 at UCSB in a 5-qubit system used to factorize the number 15 [27]. A German (Jülich, University of Munster) and Russian (Kotelnikov Institute) team proposed in early 2020 to use $YBa_2Cu_3O_7$-x nanotubes (also called YBCO, for yttrium, barium, copper and oxide, which is superconducting at 92K) to create phase qubits controllable by a single microwave photon [28]. Overall, the phase qubit seems a dead-end.

Flux Qubits: their states correspond to the direction of flow of the superconducting current in its loop. It couples a capacitor, from one to three Josephson junctions and a superinductor and has high coherence and large anharmonicity which also enable the handling of qutrits instead of qubits like what Rigetti is experimenting. Measuring the state of such a qubit uses a SQUID (superconducting quantum inter-

ference device) with two Josephson junctions connected in parallel, a magnetometer that measures the current direction in the qubit, thus its basis state 0 or 1.

This type of superconducting qubit is adopted by Rigetti, Alibaba [29], Bleximo and Atlantic Quantum in the industry vendors space. It is studied in research labs at the MIT, TU-Delft (until 2010), the Lawrence Berkeley National Laboratory (Irfan Siddiqi [30], the University of Berkeley and Yale University (Shruti Puri), the University of Maryland (Vladimir Manucharyan with a T_2 exceeding 1.35 ms and single-qubit gate fidelity over 99.99% [31,32], in Russia with a fluxonium architecture two qubits CZ gates fidelities of 99.23% [33].

In recent works, fluxonium qubits generated the best T_1/T_2 with T_1 exceeding 1 ms.[1]. They use control frequencies usually below 3 GHz which lowers down dielectric loss effects and leads to long relaxation time T_1. Single-qubit gates can have good speed in the range of 10 ns and errors levels around 10^{-4}. In this architecture, both readout and control crosstalk are expected to be small [34]. The main shortcomings of flux qubits are their bad protection from both relaxation (T_1) and dephasing (T_2) and circuit complexity for gates and readout.

The heavy fluxonium variant is using a different geometry with a 3D transmon shunted by a large linear inductance of a Josephson array [35,36]. Qubit gates can be driven by simple DC and RF flux, removing the need for complex microwave waveforming with AWG (arbitraty waveform generators) [37].

At last, in the quantum annealing domain, D-Wave is using flux controlled SQUIDs that are coupled magnetically to implement a quantum annealing process. The company has plan to implement flux qubits in a gate-based mode, with completely different chip designs.

Charge Qubits: their states correspond to current flow thresholds in the Josephson junction of the superconducting loop. Small Josephson junctions delimit a superconducting island with a well-defined electrical charge. The basis states of such charge qubits are the states of charge of the island in Cooper pairs. The most common variant is the transmon, for "transmission line shunted plasma oscillation qubit", which reduces the effect of charge noise but with a weaker anharmonicity [38]. With transmons, the Cooper pairs box is operated in the phase regime.

The nonlinear Josephson junction inductance makes the LC resonator slightly anharmonic, and its two lowest energy levels are the basis states of the qubit. Transmons are used by IBM, Google, IQM and others. To date, these are the qubits generating the lowest error rate in superconducting qubits but their low anharmonicity creates a toll on gate and readout speeds.

They are divided into at least two categories: qubits with a single Josephson junction (single junction transmon, used by IBM) or with two Josephson junctions connected in parallel (spit transmon, used by Google).[2]

Then, you have many variations with the coaxmon (OQC) and unimon (IQM) and the mergemon or merged element transmon where the Josephson junction is engineered to act as its own parallel shunt capacitor, reducing the size of the qubit [39,40]. Here, the split junction is based on a SQUID geometry, equivalent of a tunable Josephson junction. It is very convenient, but sensitive to flux noise.

Andreev Spin Qubits (ASQ) is a research-level qubit that relies on a localized microscopic excitation of the BCS condensate that natively has only two levels and is based on a nanowire. It is not a collective excitation of the superconducting loop circuit. This qubit type was proposed at and is studied at Chalmers in Sweden (funded as a H2020 program from 2019 to 2023) [43–47], Yale [48], at CEA in France [49], NBI in Denmark and also QuTech in the Netherlands, among other places. Since it manipulates electron spins in relation to a superconducting resonator and makes use of circuit electrodynamics (cQED), it sits in between the categories of superconducting and silicon spin qubits.

cat-qubits are cavity-based qubits connected to a transmon qubit used only for their preparation, readout and/or correction depending on the implementation. The cat-qubit technique was devised by Mazyar Mirrahimi and Zaki Leghtas around 2013, particularly during their work at Yale University with Michel Devoret. It was then adopted by Rob Schoelkopf's team at Yale.

Bosonic qubits is a broad category of qubits that are resilient to noise or generating less noise and make it possible to assemble logical qubits with much fewer physical qubits, in the 10–100 range instead of 1000–10,000 range [50].

It contains cat-qubits and GKP codes [51]. Other protected qubits include the zero-π qubits of Peter Brooks, Alexei Kitaev and John Preskill which use two Josephson junctions, the bifluxon [52] and other variants [53–55].

The cat-qubits approach is chosen by Alice&Bob (France), Amazon (USA) and QCI (USA) while Nord Quantique (Canada) seems to use another breed of bosonic code. Cat-qubits are also investigated in many other research labs like RIKEN in Japan. The QuCoS QuantERA collaborative 3-year European project is focused on demonstrating the scal-

[1] T_1 is the qubit amplitude coherence time, which indicates the end of coherence of the qubits linked to a loss of amplitude ("energy relaxation"). T_2 is the phase related coherence or time when some phase shift occurs, i.e. a rotation around the z axis in the Bloch sphere of the qubit state.

[2] Transmon is a diminutive of "Transmission line shunted plasmon oscillation circuit" created by Rob Schoelkopf, in other words, an oscillator circuit based on shunted Josephson junction. The shunt has become a capacitance that filters low frequencies. A plasmon is the collective behavior of free electrons of metals, here in the form of superconducting Cooper pairs.

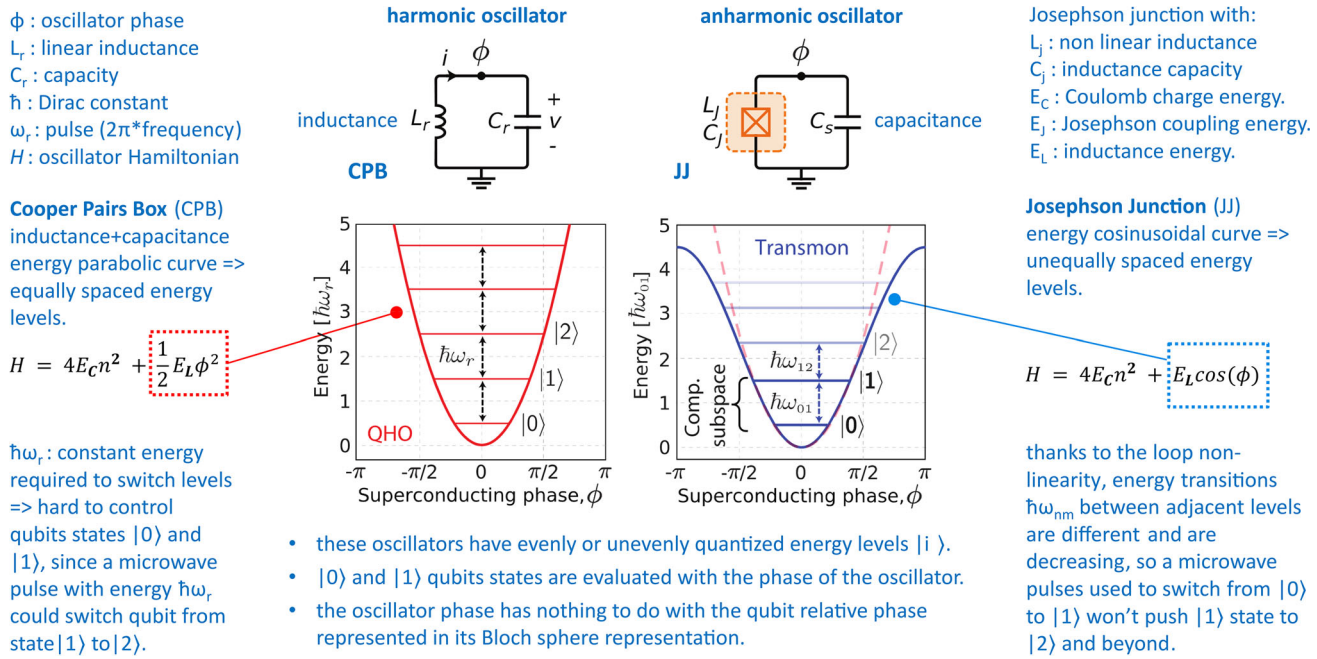

Fig. 4 Superconducting qubits use an anharmonic oscillator to differentiate two energy levels corresponding to the ground and excited state of the qubit. (cc) Ezratty [4]. Schema source in [57]

ability of cat-qubits. It combines the University of Innsbruck (Gerhard Kirchmair), ENS Lyon (Benjamin Huard), Mines ParisTech and ENS Paris (Zaki Leghtas), KIT (Ioan Pop), Inria (Mazyar Mirrahimi), the Romanian National Institute for Research and Development of Isotopic and Molecular Technologies (Luiza Buimaga-Iarinca) and Quantum Machines (Israel).

How about using superconducting qubits for implementing quantum simulations? It is not a common practice. One of the reasons is the lack of generic long-range connectivity that could enable some direct entanglement between all qubits. It would require a different physical arrangement of the qubits and to create specific long-range connections between the qubits. This is possible with using cross-resonance gates that create interactions between qubits with their respective resonance frequencies.

3 Superconducting qubit physics

We will focus here on transmon qubits that are the most common and exploited by IBM, Google and IQM. They are anharmonic and therefore nonlinear oscillators. Their nonlinearity comes from the Josephson junction which allows to better separate two energy states of the superconducting loop (*on the right in* Fig. 4) than with a simple linear resonator coupling a capacitor and an inductor (*on the left in* Fig. 4). In a harmonic oscillator, the energy levels are spaced equally and are multiples of the first energy level ($\hbar\omega_r$ in the diagram). The capacitance has an electrical energy (kinetic) and the inductance has a magnetic energy (potential). With the transmon qubit, the Josephson tunnel junction has a nonlinear inductance which creates its anharmonicity. In both cases, the flowing current is quantized with discrete energy levels corresponding to the horizontal bars in the graph in Fig. 4, with corresponding different current phases corresponding to the intersection between these bars and the parabolic (CPB) and cosinusoidal (JJ) curves. These energy states are usually controlled by microwaves pulses in the 5 GHz regime. These interactions between superconducting qubits and microwave photons are part of a branch of quantum physics called circuit quantum electrodynamics, or cQED [56].

Qubits use a linear superposition of the first two energy levels which have a different wave function relating the phase and current probabilities across the Josephson junction. The superposed states in the Bloch sphere equator like $(|0\rangle + |1\rangle)/\sqrt{2}$ and $(|0\rangle - |1\rangle)/\sqrt{2}$ correspond to an oscillating current that is dampened over time, as Rabi oscillations, in the 10 MHz range, shown in Fig. 5. The $\hbar\omega_{01}$ energy level between the basis states $|0\rangle$ and $|1\rangle$ correspond to microwave frequencies in the 4–15 GHz band (see Fig. 6).

These frequencies must be well separable from the following ones. This separation is made possible because the (microwave photon) energy sent to move from one level to the other is different from one of these levels to other higher levels. Since the upper levels are less spaced, their related transition energy is lower. As the qubits are activated by microwaves, they are no longer likely to switch to a higher

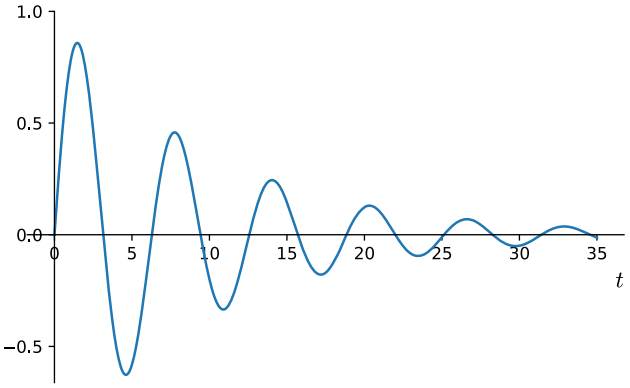

Fig. 5 The Rabi oscillation of the superconducting current representing superposed qubit states, at a frequency in the 10 MHz range

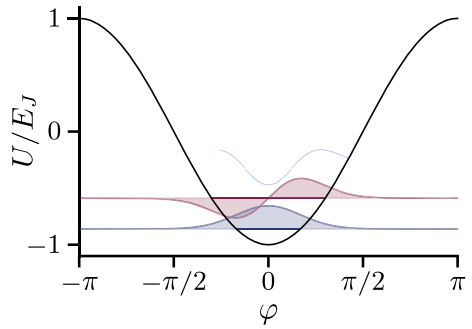

Fig. 6 $|0\rangle$ and $|1\rangle$ wave function giving the probability of phase φ in blue and green. Source in [58]

energy level. The anharmonic oscillator in the Josephson loop is provided by a nonlinear inductance L_j. The energy level between $|0\rangle$ and $|1\rangle$ of $\hbar\omega_{01}$ is higher than the energy levels needed to go to the upper levels $\hbar\omega_{12}$ and $\hbar\omega_{23}$. It is also compatible with the cooling temperature of the processor and the ambient noise.

Those of the superconducting qubits control around 5 GHz have an energy level equivalent to a temperature of about 250 mK, much higher than the 15 mK temperature commonly used. There are many rationales explaining the microwaves frequencies being used with superconducting qubits. Above 8 GHz, electronics are too expensive and below 4 GHz, the ambient thermal noise is too important. Also, the used microwaves correspond to the lowest frequency modes for which one can reach the ground state with a dilution refrigerator (see Fig. 7). But, quasiparticles in the qubit are not mainly broken by the microwaves brought in, but by higher frequencies and infrared light passing through all microwave lines or entering the cryostat, thus the need for filters, attenuators and various shielding around the qubit chipset.

The microwaves for silicon qubit control are located between 8 and 26 GHz and enable qubit temperatures of 100 mK while some can even reach 1.5 K.

There is another reason for running the qubit at around 15 mK. It takes a certain amount of energy, known as the energy gap, to break up the Cooper pairs running in a superconducting qubit. In aluminum that is the typical material used to create the Josephson junction and its surroundings, the energy gap corresponds to 90 GHz at 20 mK. It is an order of magnitude greater than the energy difference between the two levels in a qubit. It means that the qubit can be driven with lower energies (in the 4–8 GHz range) without breaking up the superconducting current Cooper pairs and altering the quantum coherence of the qubit [59].

What differentiates phase, charge (transmon) and flux qubits are the relative values of the charge energy (E_C, *aka* Coulomb charge energy), the Josephson coupling energy (E_J) and the qubit inductance energy (E_L) as shown in Fig. 8 [60].

Then, just with transmon qubits, you find other variations with:

- Fixed (IBM, MIT) or tunable (Google) qubit frequencies.
- Tunable couplers to entangle several qubits (Google, IBM, IQM).
- Architectures mixing digital and analog superconducting computing [62].
- Controlled-phase gates with variable amplitude and frequency which could significantly reduce the depth of quantum circuits particularly for implementing a quantum Fourier transform required in many algorithms like Shor, HHL and QML (C-R_θ) [63].
- New techniques to implement faster qubit readout [64, 65].
- And techniques using qutrits instead of qubits (with Rigetti, although with fluxonium qubits).

Of course, many researchers are looking for ways to improve qubits fidelities with better materials and designs [66].

The qubit itself is coupled to a cavity containing a resonator usually implemented as a coplanar waveguide (CPW) resonator on a superconducting circuit. Its length usually corresponds to a quarter-wavelength or the resonator drive frequency. With a 6 GHz drive frequency, it turns into a 1.25 cm resonator that is usually squeezed in a serpentine layout.

The energy of the ensemble is modelized by a Jaynes-Cummings Hamiltonian as shown in Fig. 9 [67]. This involves many notions like a Jaynes-Cummings spectrum, a resonant regime (the cavity-qubit are interoperating oscillators), dressed states (the different energy levels of the qubits) and a dispersive regime (enabling qubits readout with the resonator) [68].

Many parameters define a superconducting qubit's characteristics, like its Q factor, the ratio between the energy stored in an oscillator and the energy dissipated per oscillation cycle

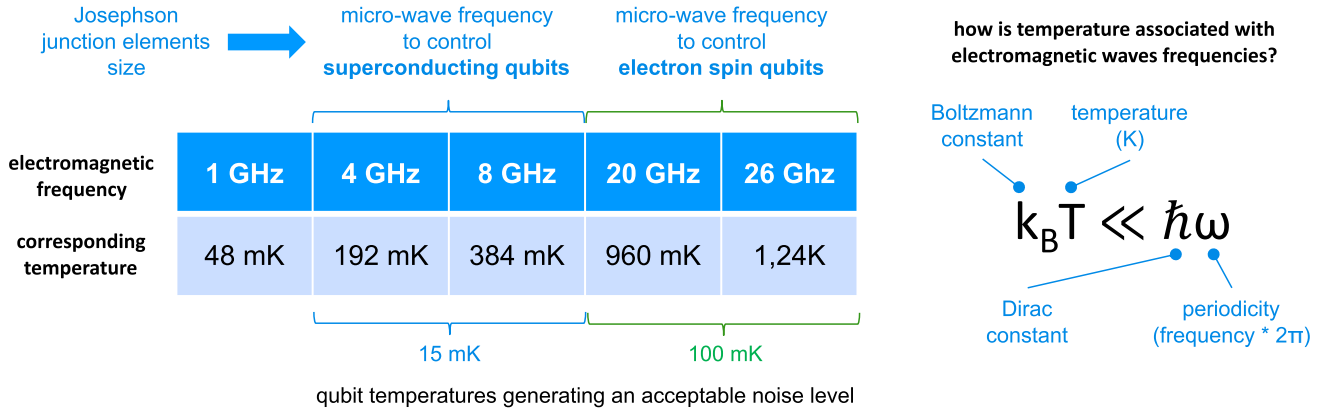

Fig. 7 The rationale behind the 15 mK operating temperature of superconducting qubits and higher temperatures with silicon-based electron spin qubits. (cc) Ezratty (2021)

Fig. 8 Periodic table of superconducting circuits showing how various types of qubits differentiate according to the relative ratios between the charge energy ($E_{C,}$), the Josephson coupling energy (E_J) and the qubit inductance energy (E_L). Source in [61]

E_J/E_C \ $E_L/(E_J-E_L)$	0	$\ll 1$	~ 1	$\gg 1$
$\ll 1$	cooper-pair box			
~ 1	quantronium	fluxonium		
$\gg 1$	transmon			flux qubit
$\gg\gg 1$			phase qubit	

Table 1: "periodic table" of superconducting quantum circuits

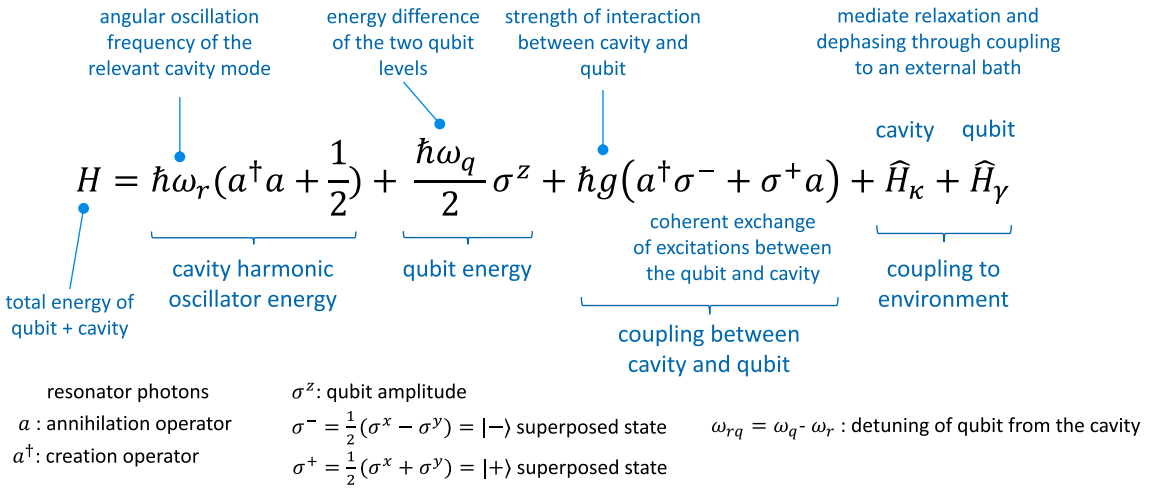

Fig. 9 The Jaynes–Cumming cQED Hamiltonian describes how a superconducting qubit exchange photons with its surrounding cavity. Here the cQED are in the microwaves regime. (cc) Ezratty [4]

times 2π. It characterizes the stability of a superconducting qubit and determines its T_1 or relaxation time. The greater the Q factor is, the longer T_1 will be but it can be detrimental to noise sensitivity [69].

4 Superconducting qubit operations

The general principle of superconducting qubits operations is as follows:

Qubit quantum state in the generic case of a transmon is a two-level charge of Cooper pairs that correspond to a nonlinear oscillator containing at least a Josephson junction and a

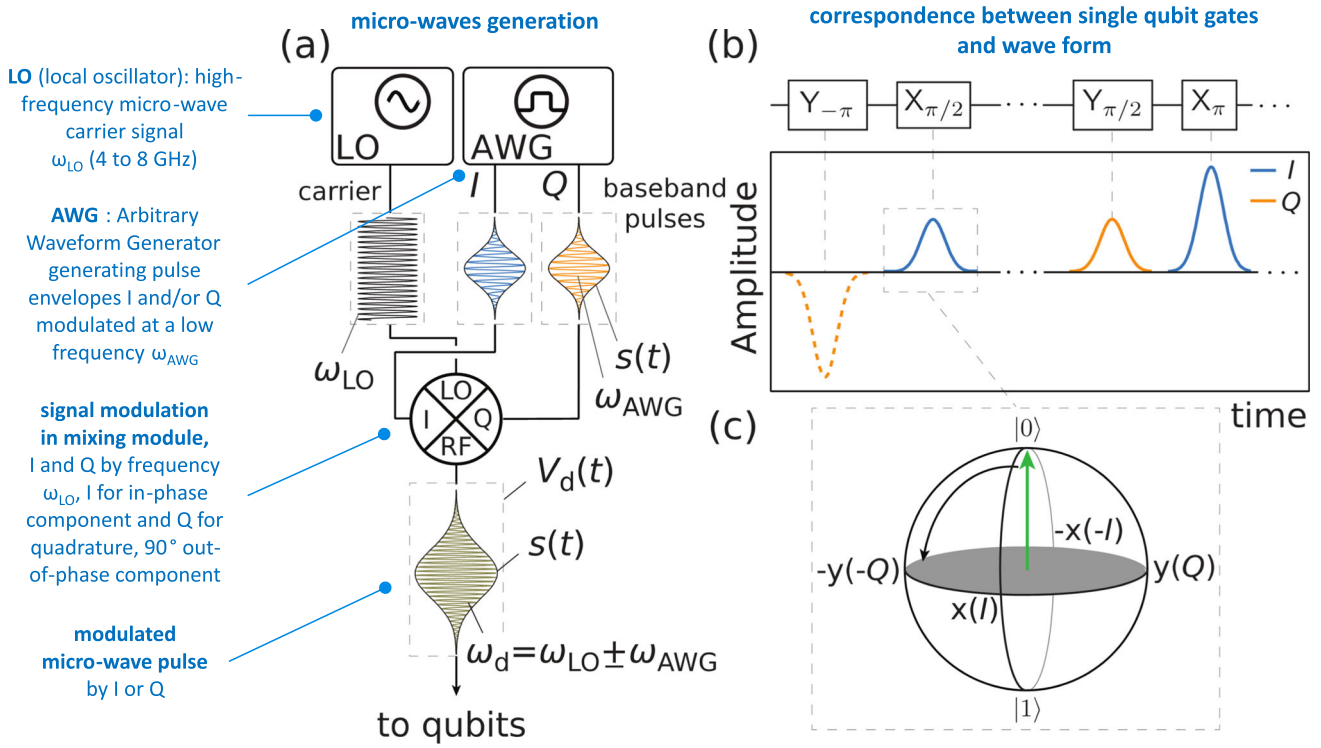

Fig. 10 Single qubit gates drive microwaves generation. The AWG generates pulse waveforms for in-phase and quadrature signals that are then mixed with a local oscillator pulse (LO). It create a modulated micro-wave pulse that is used to drive single qubit gates depending on the ratio between in-phase and quadrature signals. Source: [70]

capacitance laid out in a current loop. A flux bias (direct current pulse) can be used to individually control each qubit resonant frequency if it is frequency tunable. It can help reduce control frequency crosstalk between qubits but at the cost of a lower lifetime (T_1). It is better to have fixed and different qubit frequencies.

Single-qubit quantum gates are generated by microwave pulses sent via coaxial cables on the qubits (Fig. 10). Their frequency is adjusted to the energy level $\hbar\omega_{01}$ mentioned above. This frequency is calibrated to be different on adjacent qubits to avoid crosstalk effects. The microwave pulse amplitude controls the rotation angle and its phase adjusts the axis of the gate rotation operation. This makes it possible to create T, S and R gates with a phase other than a quarter or half turn in the Bloch sphere. In practice, two arbitrary waveform generators create a wave form for "in-phase" and "quadrature" (I and Q) signals which are two microwave pulses that have the same (local-oscillator originated) frequency and are 90° out of phase, as shown in Fig. 11. The I signal is a cosine waveform and the Q signal is a sine waveform. They add-up in the mixer to create a pulse signal with an arbitrary phase depending on the relative amplitudes of the I and Q waveform signals [71]. The mixer then adds the local oscillator signal to the resulting signal. At 5 GHz, an LO pulse lasts 0.2 ns. Most single qubit gate last at least 10–20 ns. It means in that case that a generated microwave packet contains about 50 to a hundred 5 GHz pulses shaped by its wave form. Microwave pulses generated at ambient temperature are progressively attenuated and filtered at every stage of the cryostat so that only a couple hundred microwave photons reach the qubit. The attenuators eliminate photons proportionally to the cooling budget available at each cold plate stage.

Two-qubit quantum gates are realized with a coupling circuit positioned between the two qubits, which can be a simple capacitor or a dynamically controllable system. Depending on the implementation, there are various types of two-qubit gate like $\sqrt{iSWAP}$ or the CZ gate. As we will see later, this coupling is managed with an intermediate qubit in Google's Sycamore processor and their Chinese equivalents. IBM is not using couplers but instead cross-resonance gates.

Qubits readout depends on its type. With transmon qubits, a resonator is coupled to the qubit. It transmits a microwave pulse in a resonator that is coupled with the qubit using microwave reflectometry. The qubit state slightly affects the resonator frequency and phase. These readout microwaves are usually amplified in several stages. The method is called "dispersive readout" where for a fixed microwave drive frequency, the resonance frequency of the waveguide resonator shifts depending on the qubit measured state. This measurement technique protects the qubit from all radiations except

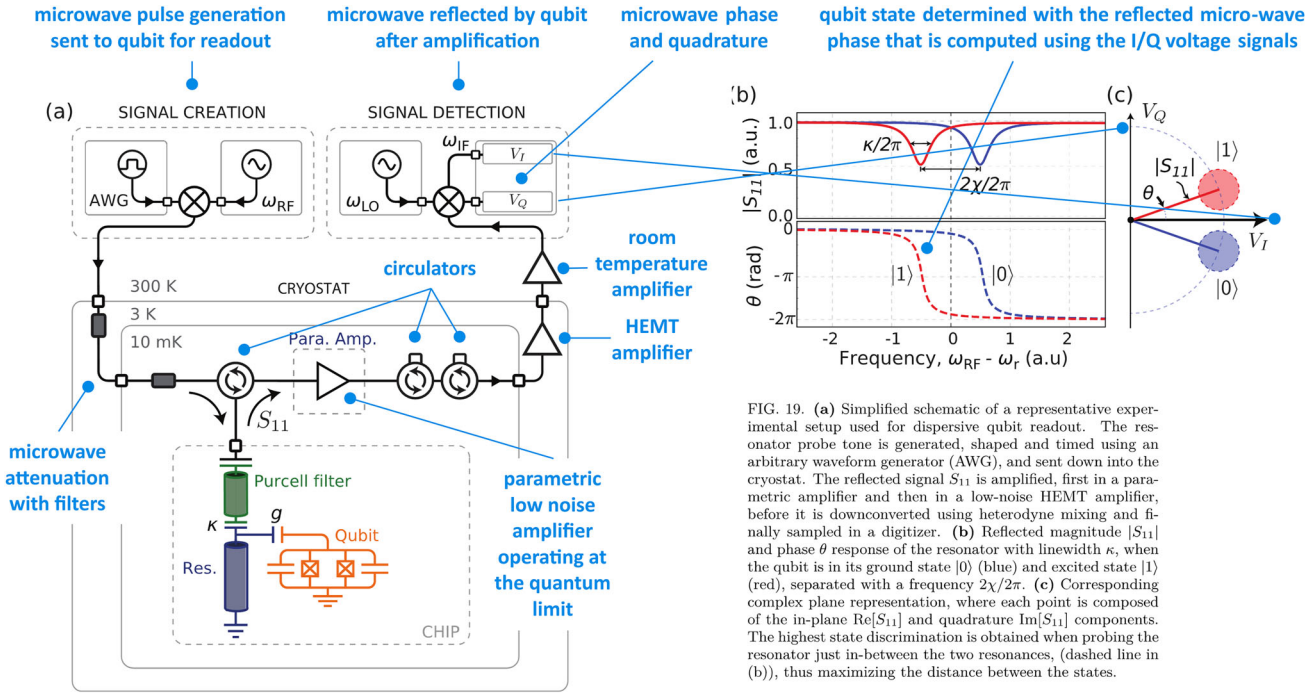

FIG. 19. **(a)** Simplified schematic of a representative experimental setup used for dispersive qubit readout. The resonator probe tone is generated, shaped and timed using an arbitrary waveform generator (AWG), and sent down into the cryostat. The reflected signal S_{11} is amplified, first in a parametric amplifier and then in a low-noise HEMT amplifier, before it is downconverted using heterodyne mixing and finally sampled in a digitizer. **(b)** Reflected magnitude $|S_{11}|$ and phase θ response of the resonator with linewidth κ, when the qubit is in its ground state $|0\rangle$ (blue) and excited state $|1\rangle$ (red), separated with a frequency $2\chi/2\pi$. **(c)** Corresponding complex plane representation, where each point is composed of the in-plane Re$[S_{11}]$ and quadrature Im$[S_{11}]$ components. The highest state discrimination is obtained when probing the resonator just in-between the two resonances, (dashed line in (b)), thus maximizing the distance between the states.

Fig. 11 Superconducting qubit readout process. It starts with another micro-wave pulse generation as seen in figure that is sent on a resonator nearby the qubit. This will create a non-demolition measurement of the qubit and generate a reflected micro-wave pulse. It will traverse circulators and a low temperature low-noise parametric amplifier. The circulators prevent the amplified microwave pulse to create some back-action on the qubit itself. This pulse is then amplified two more times at around 4 K and at ambient temperature, and demuxed and converted in digital format for subsequent analysis. Source: [69]

the readout microwave pulse at ω_r, it amplifies the outgoing signal with the lowest added noise (near the quantum limit). The readout also creates a differentiated phase in the reflected microwave that is analyzed after demixing which generates the in-phase and quadrature signals (I/Q). Measuring the phase of the reflected microwave determines the state of the qubit after measurement without destroying it. It's a QND readout as already explained (see Fig. 11).

One first stage can use a low-noise superconducting Josephson Parametric Amplifier (JPA) or Traveling Wave Parametric Amplifier (TWPA) operating at the quantum limit, then with a high electron mobility transistor (HEMT) amplifier running at the 4K stage and, at last, with a Low Noise Amplifier (LNA) running at room temperature. TWPAs play a key role with enabling frequency-domain multiplexing of qubit readout, thanks to a bandwidth that can exceed 2 GHz. The most advanced TWPAs are made at the MIT-Lincoln Labs in Will D. Oliver's lab. Industry vendors also provide TWPAs like LNF (Sweden) and Silent Waves (France). IBM and Google design and manufacture their own TWPAs.

At last, the amplified microwave is converted in digital format with an ADC (analog to digital converter) and analyzed by a FPGA circuit to identify the qubit basis states $|0\rangle$ or $|1\rangle$ with a microwave phase analysis.

Frequency-based multiplexed readout can also be achieved to simplify the wiring exiting the qubit chipset. The readout microwave is modulated with a higher frequency than the quantum gates frequency, above 6 GHz. Other techniques for measuring the state of superconducting qubits are being considered, such as the activation of qubit fluorescence. It is done by jumping from the $|0\rangle$ to $|2\rangle$ state of the qubit, the transition to the $|1\rangle$ state not being possible with the fluorescence excitation photon [72].

Connectivity is an important feature of a quantum processor. The more qubits are connected with each other, the fewer SWAP gates must be run to logically entangle them. Il can also contribute to make error correction codes more efficient and use a lower overhead of physical qubits, like with the LDPC codes [73]. With 2D structures, one of the problems to be solved lies in the internal connections in the chipset. 3D architectures are used with one layer for qubit readout and another for qubit operations but the qubits topology connectivity is at best with four nearest neighbors like with Google's Sycamore. IBM is using a "heavy hex lattice" connectivity since 2021. Using hexagonal unit cells of 12 qubits with 1-to-2 and 1-to-3 connectivity, it generates better qubit gate fidelities and enables error correction codes implementation. A new approach consists in using multiple metal layers connectivity chipsets that are connected to the qubit chipset with

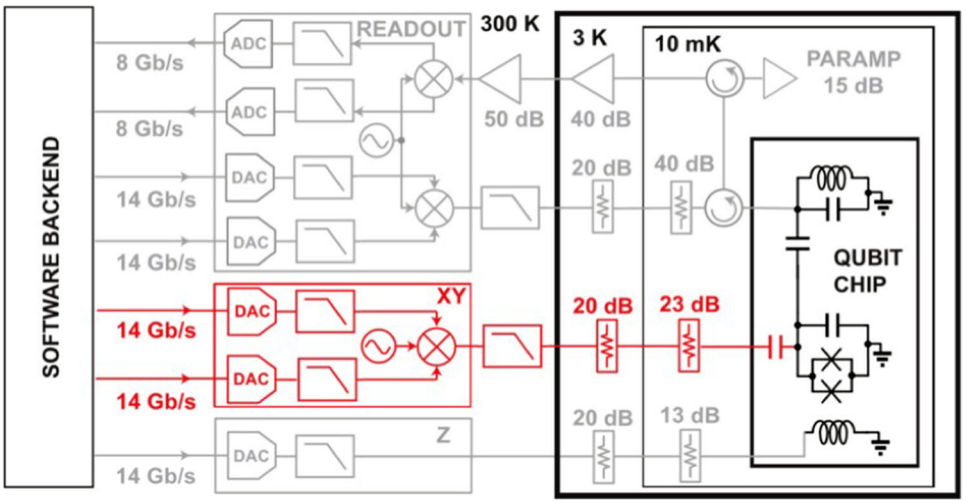

Fig. 12 Sycamore's qubit control and readout architecture showing the 4 cables driving a qubit. Z gates are driven by pulsed DC (direct current) signals while X and Y gates are driven by pulsed micro-waves. Notice the volume of data getting in the DACs (digital-analog converters) and out of the ADCs (analog to digital converters). Source: Google

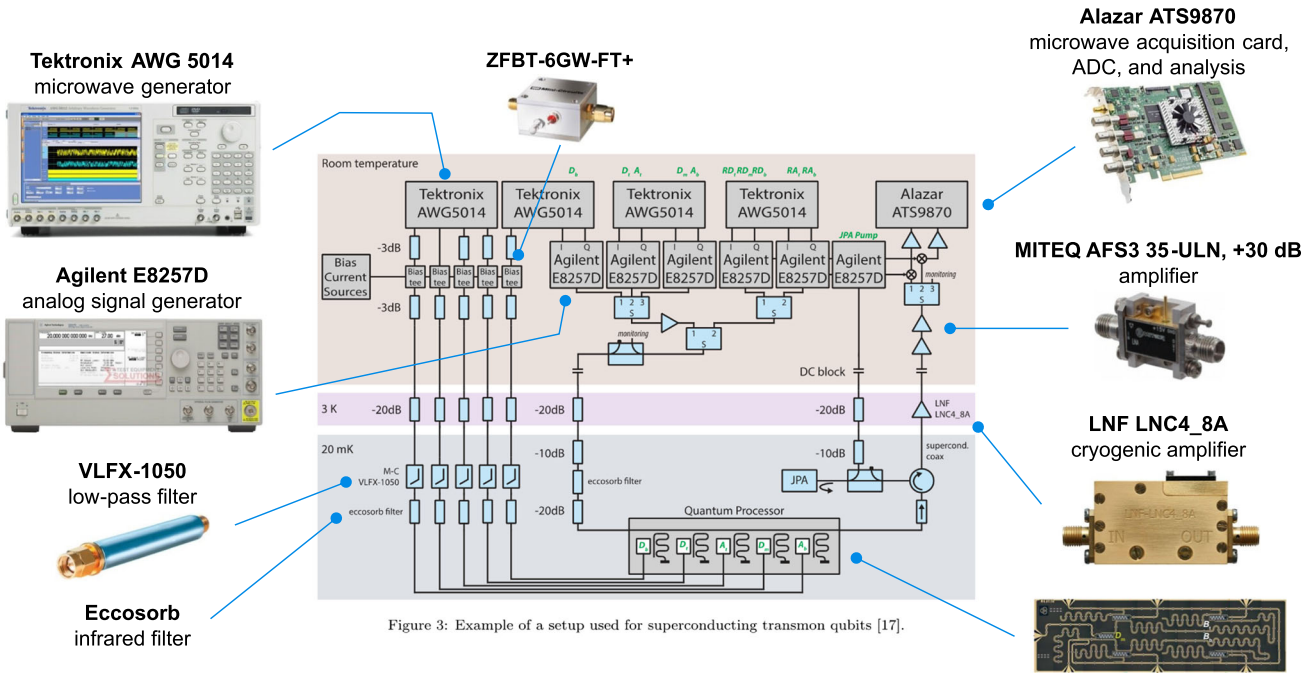

Fig. 13 A typical superconducting qubits lab configuration. I have added visuals of the electronic components used in the configuration to a schema found in [74]. Nowadays however, labs working on actual QPUs use more dedicated and integrated qubits control technologies from industry vendors (Quantum Machines, Zurich Instruments, Keysight, Qblox, etc)

through-silicon vias (TSVs) vertical connectors. The most recent designs from IBM and the MIT Lincoln Labs have between three and seven metal layers.

5 Superconducting quantum computing setups

In the current state of the art, the cryostats housing these qubits are filled with many cables and microwave attenuators driving the qubits and with first stages amplifiers used in the qubits state readout. There are about 4–5 cables per physical qubit which creates a certain burden to overcome in scalable quantum computers, as shown in Fig. 14.

Implementing quantum error correction will require thousands of physical qubits per logical qubit, a number that depends on several parameters like the physical qubits fidelities, their connectivity, and the logical qubit target fidelities which can range between 10^{-6} to 10^{-19} depending on the algorithms. Quantum chemical simulation algorithms are particularly demanding here. With usual error correction codes like surface codes that implement fault-tolerance corrections, the key determinant of physical qubit overhead is also the number of T gates in the algorithm since these gates are the most expensive to correct. It will create significant challenges for scaling up the architecture at least, with

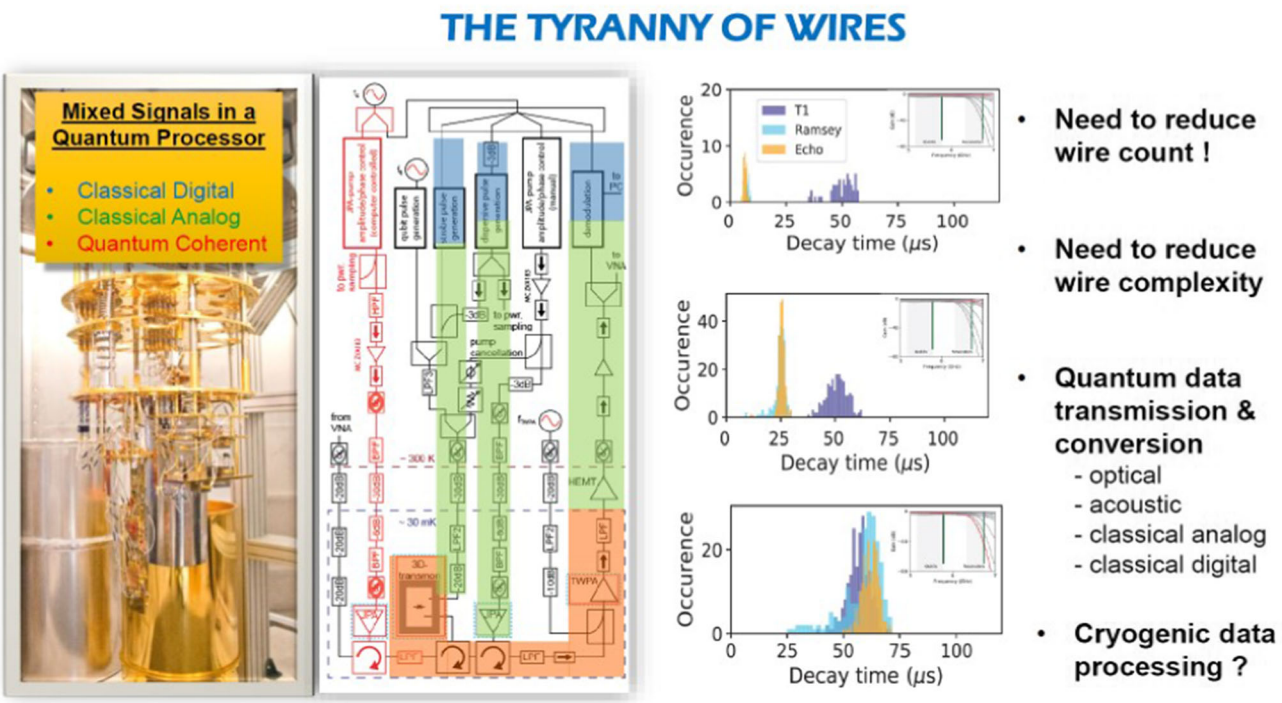

Fig. 14 The tyranny of wires in superconducting qubits. When QPUs will reach thousand of qubits, it will require innovative multiplexing solutions. Source: [77]

the existing cabling and external microwave generation and readout systems.

Digital-to-analog converters (DACs) and Analog-to-Digital converters (ADCs) convert microwaves at room temperature and handle a very large volume of outbound or inbound data of 8–14 Gbits/s as shown in the diagram in Fig. 12 corresponding to Google's Sycamore.

This data is managed in real time. It does not however seem necessary to store it. It is not a big-data system!

The electronics used in research laboratory equipment is illustrated with the example in Fig. 13 of a configuration used to test a 5-qubit superconducting chipset in 2015.

Its uses classical off-the-shelf equipment from Rohde & Schwarz or Tektronix. These external generators are appreciated for the quality of the microwave pulses they produce. For a larger number of qubits, multiple microwave generators are used from vendors like Zurich Instruments, Keysight, Qblox and Quantum Machines (which was developed initially at Yale in the USA). These solutions are not yet very scalable. It pushed IBM to develop they own qubit control electronics with 433 qubits control fitting in a single rack of electronics for their Osprey system presented in November 2022.

Others, like SeeQC, are attempting to miniaturize all or part of these components with superconducting electronics which have a much lower power drain and can work within the cryostat.

Superconducting qubits fidelities are not best-in-class compared to trapped ions. There is some progress being made to reduce qubit noise. The noise has several origins such as charge fluctuations, random electrons, materials impurities and crosstalk between distant qubits. Qubit fidelities are currently not high enough to implement error correction codes. Also, various methods are proposed to improve readout fidelity [75,76] (Fig. 14).

The size of superconducting qubits is in the micron range, making it difficult to create large chips with millions of qubits. Miniaturization always seems possible but it is difficult to manage because the quality of the superconducting qubits seems to decrease with a smaller size [78,79]. As a consequence, most vendors like IBM, plan to create chipsets up to about 133 qubits and then connect several of these chipsets with microwave guides and/or entangled phototonic links able to convert qubit quantum states to photonic quantum states. These various quantum processor interconnect currently have a very low TRL (technology readiness level).

6 Superconducting qubit chipsets manufacturing

Superconducting qubits are electronic circuits built with techniques that are not that far from how classical analog circuits are being produced like in the radar and electronics markets, with some similarities with digital electronics, *aka* CMOS chipsets.

Materials used for manufacturing superconducting qubits include generally aluminum (for the Josephson junction, at least for the dielectric), niobium (for capacitors and resonators and sometimes the Josephson junction) and indium (for the chipset connectors), bore (in boron-nitride in Josephson junction dielectric, titanium nitride (for capacitors, with a better quality factor) and occasionally selenium (associated with niobium and bore in capacitors), silicon or sapphire (for the wafer substrate) and tantalum (see Fig. 15). As presented at the APS March meeting in Las Vegas in March 2023, the MIT Lincoln labs showed good results with hydrofluoric acid treatments of the Josephson junction for cleaning surfaces, using aluminum on silicon substrates. These various advances still have to be embedded in industry vendor processors.

While most deposition techniques generate polycrystalline structures, some are starting to investigate epitaxial deposition to create monocrystalline structures. IMEC in Belgium already tests such processes avoiding lift-off and angled evaporation, all done with photolithography. They are part of the related EU project Matqu with CEA-Leti and others to build superconducting qubits on 300 mm wafers using existing CMOS fabs. Although it didn't generate improved qubit fidelities compared to state of the art, IMEC expects to obtain better results with future prototypes.

Superconducting qubits miniaturization is an interesting area of research given they are currently quite large, mainly due to the size of their resonators with a length of $\lambda/4$, λ corresponding to their control wavelength. It can exceed a surface of 1 mm^2. Resonators could be as small as 0.04 mm^2 using special fabrication techniques [81,82]. Another option would be to have remote resonators and an X-Y addressing scheme like with classical RAM, but with the inconvenience of serializing gate operations, and slowing down computing.[3]

Another area of research deals with improving the connectivity between superconducting qubits using 3D circuits, with secondary chipsets providing the connectivity underneath the superconducting qubit circuit and interconnect coming from separating qubits from microwave controls, using TSV (through-silicon vias) as developed by IBM (see Fig. 16).

7 Superconducting qubit current research

A significant number of research laboratories are working on superconducting qubits all over the world. In the USA, at Yale University and MIT, in Europe and in Germany, in Sweden at the WACQT of Chalmers University, in France at the CEA, in Switzerland at ETH Zurich, in Finland and in Japan. In the industry, IBM, Google, Amazon and Alibaba also have strong research teams working respectively on transmon, transmon and fluxonium qubits on top of many startups.

Other works aim at lengthening the coherence time of superconducting qubits, notably at Princeton in Andrew A. Houck's team. Indeed, this coherence time of the order of one hundred micro-seconds (μs) is still quite limiting. It generates a constraint on the number of quantum gates that can be executed in a quantum software, even if the accumulated errors become prohibitive before this limit threshold. New records were broken in 2021 with 1.6 ms T_1 at Princeton and Sherbrooke with a 0-π circuit (but with a 25 μs dephasing time, aka T_2) and 210 μs with transmon qubits at Yale. In May 2021, a China team obtained a 300 μs T_1 with a transmon qubit. IBM reached the 1 ms T_1 barrier with one experimental planar transmon qubit in May 2021 as well (but the related paper is still pending). The best lab-level record was with a 1.48 ms T_2 coherence time on flux qubits at the

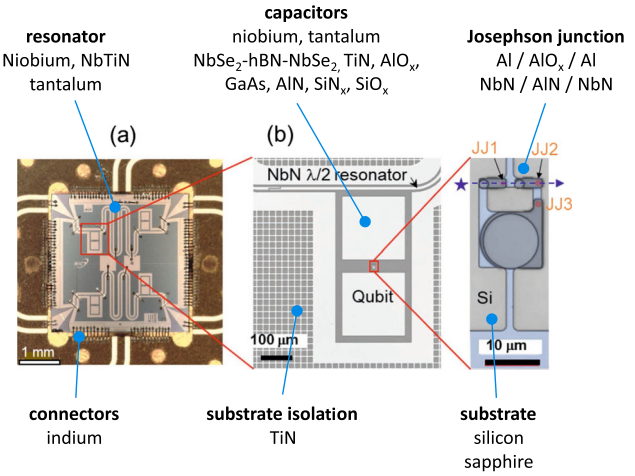

Fig. 15 The various components and materials used in a superconducting qubit. Source: [80]

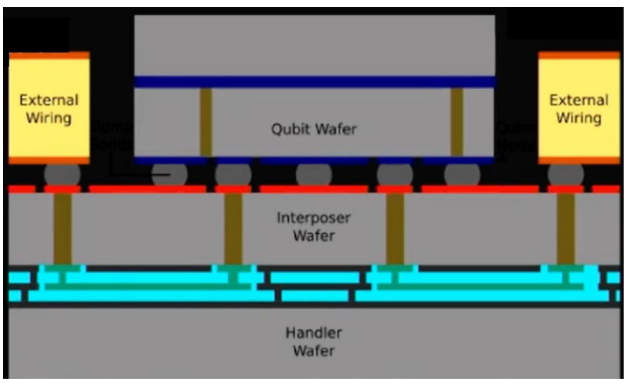

Fig. 16 The three stacked die chipset architecture used in Eagle's 127 qubit processor. Source: IBM

[3] An X-Y addressing scheme would route signals to the qubit resonators from the edge of the chipset, X and Y corresponding to two orthogonal edges. You would then polynomialy reduce the number of resonators from N to $\sqrt{N}$ with N being the number of qubits of a square matrix layout chipset.

Fig. 17 The huge SRF superconducting qubits from the DoE Fermilab. Source: [84]

University of Maryland in Vladimir Manucharyan's team. These records are however not necessarily obtained with a great number of functional qubits... when more than 2 are used!

Superconducting qubits lifetime record is still way above this, with 3D SRF cavities (for superconducting radio frequency cavities). These are developed by the DoE Fermilab and have a very high Q-factor. In 2020, they reached qubit lifetimes of about 2 s with special materials design reducing the two-level system losses. Fermilab researchers plan to implement qudits with these SRFs, packing between 63 and 128 effective qubits into nine SRF cavities hosting qudits. These cavities are bulky, the size of the device being about one meter long in Fig. 17 [83].

Other researchers work on using various qubits materials like titanium nitride and tantalum on sapphire substrates, at Princeton, ENS Lyon and Alice&Bob among other locations. These are used in complement to the Al/AlO/Al Josephson junctions, for various other parts of the qubit circuits (isolators, capacitances, resonators).

As with many solid-state qubits, one of the key research goals is to convert superconducting microwave photons into photons in the visible/infrared band to allow their long-distance transport and entanglement sharing, in particular via fiber optic-based telecommunication, which would become the basis of distributed quantum computing and so-called scale-out architectures. This is envisioned by many players like IBM to overcome the difficulty to scale superconducting qubits on large chipsets. It however bring its load of challenges given it is difficult to create deterministic entangled sources of photons and connect these to qubits across several chipsets.

There is another interesting field of research aimed at simplifying qubit readout that may avoid the burden of parametric microwave amplification and the bulky circulators used at the 15 mK stage. One of these consists in using microwave photons counting and Josephson photomultipliers (JPM) that are embedded directly in the qubit chipset [85]. It has however some shortcomings to overcome like crosstalk and loss of qubit fidelity over time.

In 2021, a China research team led by Jian-Wei Pan created a 66 superconducting qubits system and claimed having reached another quantum advantage. In this Zuchongzhi 2.1 system, they reproduced the Google supremacy experiment with a 2D array of qubits with 13 additional qubits, using the same coupling technology, with 110 couplers [86]. Their fidelities were not best-in-class with 99.86% for single qubit gates, 99.24% for two-qubit gates and 95.23% for qubits readout, on top of a rather low T_1 of 30.6 μs. In their experiment, though, they did use only 56 of their 66 qubits, showing that qubits fidelities are probably not that good when all qubits are activated. In September 2021, they used 60 qubits on 24 cycles with an improved readout fidelity of 97.74% [87].

8 Market readiness and use cases

The current generation of superconducting gate-based quantum computers belong to the pre-NISQ and NISQ classes. NISQ stands for noisy intermediate scale quantum computers. It describes quantum computer with over 50 physical qubits that can bring some advantage when compared to best in class classical computers. These advantage can be about computing speed, quality of results and some energetic advantage. Pre-NISQ systems have below 50 qubits and are usually below the quantum advantage threshold.

NISQ systems use quantum algorithms that are more or less resilient to noise and must be shallow, meaning, have a low number of quantum gate cycles. A rule of thumb formula dictates the fidelities required for a given algorithm as below with ϵ being the system two-qubit gate error rate, n being the number of used qubits and d the quantum algorithm depth.

$$\epsilon = \frac{1}{n * d} \tag{8.1}$$

Running a quantum algorithm with 50 qubits and a depth of 10 gate cycles would thus require qubit fidelities (1-ϵ) above 99.8%. If you raise the bar to 100 qubits, you need fidelities of 99.9%. And if the algorithm is not shallow with, say, 100 gate cycles, you're in for a requirement of 99.99% fidelities. The typical class of algorithms suitable to NISQ platforms are variational algorithms using an ansatz preparation done by a classical computer to compute a system Hamiltonian and adjusted across many runs to minimize an objective function.

These algorithms belong to three main classes: varional quantum eigensolver (VQE) to compute many-body quantum systems Hamiltonians, quadratic unconstrained binary optimizations algorithms (QUBO) to solve combinational optimizations and quantum machine learning (QML) for various machine learning classification, automatic clustering and prediction tasks.

The scatter plot in Fig. 19 describes the current landscape of industry vendors superconducting quantum computer with charting two-qubit gate fidelities and qubit numbers, in log scales. It shows that so far, no computer sits in the usable

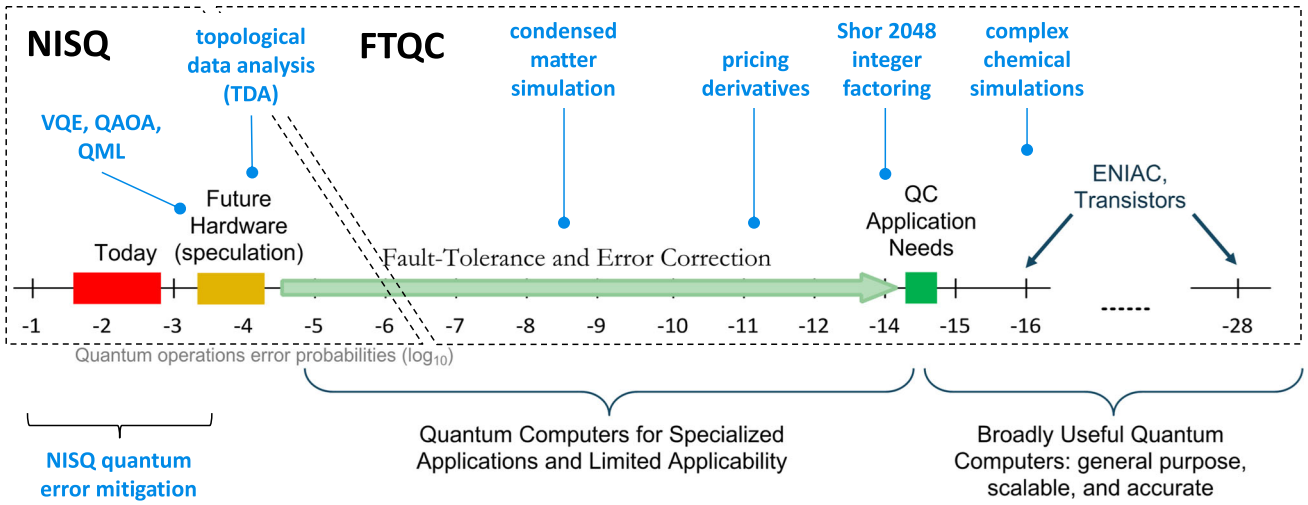

Fig. 18 How NISQ and FTQC may overlap with competition between NISQ and quantum error mitigation extending the capacities of noisy qubits while corrected qubits will enable FTQC and greater depth algorithms. Source: Bert de Jong (Department of Energy) and additions by Ezratty (2023)

NISQ zone. Some vendors like IBM are planning to release new QPUs (quantum processing units) with fidelities in the 99.9% range, sufficient to run NISQ quantum algorithms with some quantum advantage. But as shown in Fig. 18, we may have an overlap between NISQ and FTQC with regards to algorithms depth capabilities, with competition between very high fidelity qubits and quantum error mitigation vs large numbers of high fidelity qubits and quantum error correction.

Another often untold challenge is with the measurement of the "expectation value of observables" of the Hamiltonian resulting from the quantum part of these variational algorithms. On a theoretical basis, it requires an exponential number of quantum circuit shots which is not acceptable past 40 qubits. Many methods are thus designed to avoid this exponential curse [88]. This is however not specific to superconducting qubits.

The current period is however fruitful for using existing NISQ hardware. It serves the purpose of learning to program these systems, to design new algorithms and to create various error mitigation techniques. It also provides a feedback loop to quantum computers developers, noticeably around the various software cloud tools managing these QPUs (Fig. 19).

Beyond or in parallel with NISQ systems development is the rather long-term advent of so-called fault-tolerant quantum computers (FTQC). These QPUs will rely on groups of logical qubits with error rates that are reduced thanks to the use of quantum error correction codes and redundancy. Logical qubits will have a lower error rate depending on the error correction codes, the physical qubit fidelities, their connectivity and their number. It is expected that superconducting-based logical qubits will require between a thousand to millions of physical qubits depending on the target application error rate. This target error rate depends again on the depth and breadth of the user quantum algorithm and is not necessarily static in a given QPU. The algorithms logical qubit fidelities requirements ar usually inversely proportional to the their number of T gate (phase rotation gate of 1/8th of a turn). The typical FTQC algorithms bringing an exponential speedup use a lot of T gates to implement the quantum Fourier transform (QFT) primitive. This primitive is used in quantum phase estimate and quantum amplitude estimates (used in many-body simulations), linear algebra algorithms and integer factoring algorithms.

9 Challenges ahead

Like all qubit types, superconducting qubits have their challenges to enable the creation of useful quantum computers, whether in the NISQ or FTQC realm. On paper, the technology could scale to thousands if not millions of qubits. The best-in-class fidelities were obtained by IBM with its Egret 33-qubit processor in November 2022 showcasing a 99.7% two-qubit gate fidelity. Creating a fault-tolerant quantum computer would require at least about 100,000 physical qubits with a 99.9% fidelity. This would enable 100 logical qubits and an equivalent computing depth.

These requirements create immense challenges: can qubit crosstalk be contained at this scale? Is it possible to maximally entangle so large many-body quantum systems in a controlled way ? How to design quantum error correction codes with a minimum physical qubit overhead and fidelities requirements? Is it possible to create adequate low-power control electronics, cabling, multiplexing and cryogenics to reach such a scale [89]? Will the related energy consumption

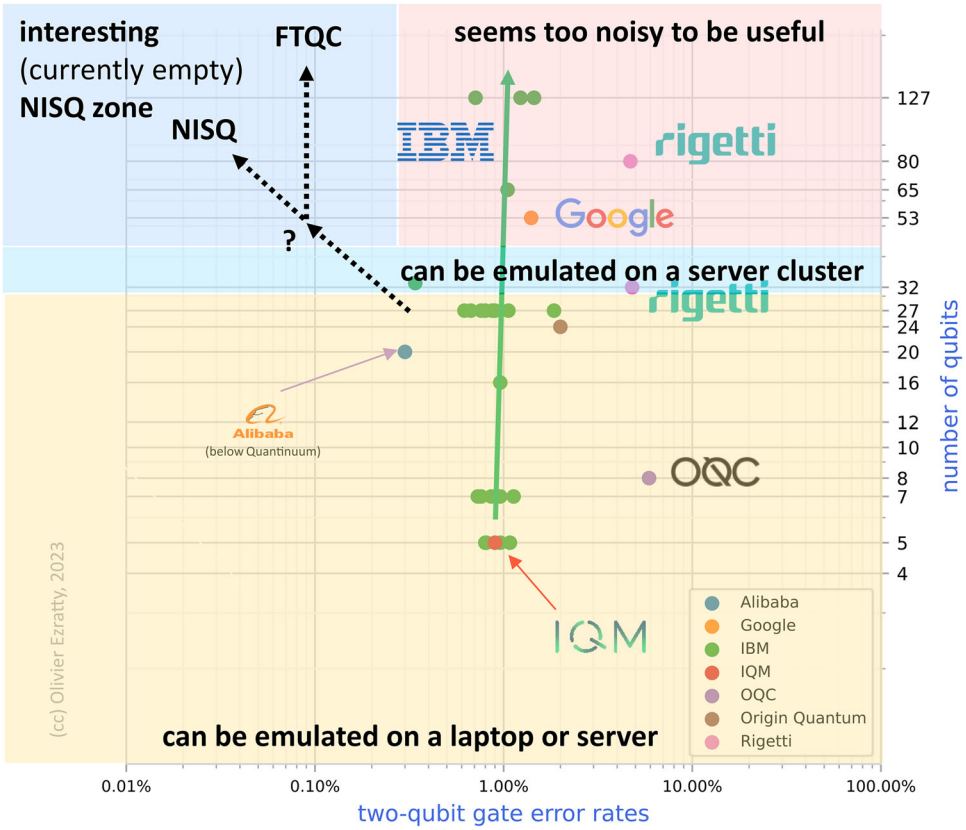

Fig. 19 Current two-qubit gate fidelities of superconducting qubit computers from commercial vendors. The blue zone corresponds to the area where QPUs could bring some computational advantage either in the NISQ or in the FTQC regime. The FTQC regime requires at least 99.9% fidelities and scale to millions of qubits while the NISQ regime is based on a few hundreds or thousands of qubits. Source: vendors data and compilation by Ezratty (2023)

be contained, an interdisciplinary question that the Quantum Energy Initiative proposes to address in a systemic way [90,91]? Will it be possible to interconnect several quantum processors with microwaves or entangled photon resources? All of these scientific and technology challenges are gigantic.

Another challenge is to improve the software tools used to design these qubit chipsets. Electronic Design Automation tools (EDAs) run on classical computers. There a few tools to design and digitally simulate qubit chipsets but they are not yet enough integrated. Among these is Qiskit Metal from IBM. It was announced in 2021 and is currently in alpha version. In February 2023, Amazon AWS introduced Palace (PArallel, LArge-scale Computational Electromagnetics), a finite element open source code for full-wave electromagnetics simulations capable of simulating a single transmon qubit with its readout resonator coupling and a terminated coplanar waveguide (CPW) transmission line for input/output. Other spare Python frameworks are used to simulate at various abstraction levels a qubit chipset from the inner working of the qubit up to the whole integrated chipset.

In the meantime, vendors like IBM, Rigetti and Google try to create NISQ systems with hundreds of qubits that may bring some quantum computing advantage thanks to the technique of quantum error mitigation that works with shallow depth algorithms, particularly variational ones working in hybrid mode along with supercomputers. Creating usable NISQ systems would still require much higher gate fidelities than available today with two-qubit gate fidelities superior to 99.99%.

Data Availability Statement This manuscript has no associated data or the data will not be deposited. [Authors' comment: There is no data provided with the paper since this is a review paper, not a paper with specific experimental results.]

References

1. M. Kjaergaard et al., Superconducting qubits: current state of play. Annu. Rev. Condens. Matter Phys. **11**(1), 369–395 (2020). https://doi.org/10.1146/annurev-conmatphys-031119-050605
2. S. Xu et al. Digital simulation of non-abelian anyons with 68 programmable superconducting qubits. arXiv (2022). https://doi.org/10.1103/RevModPhys.92.015003
3. J. Martinis, M. Devoret, J. Clarke, Energy-level quantization in the zero-voltage state of a current-biased Josephson junction. Phys. Rev. Lett. (1985). https://doi.org/10.1103/PhysRevLett.55.1543
4. O. Ezratty, Understanding quantum technologies 2022, arXiv (2022). https://doi.org/10.48550/arXiv.2111.15352
5. P.W. Anderson, J.M. Rowell, Probable observation of the Josephson superconducting tunneling effect. Phys. Rev. Lett. (1963). https://doi.org/10.1103/PhysRevLett.10.230
6. Y.. Nakamura, Y.. Pashkin, J..-S.. Tsai, Coherent control of macroscopic quantum states in a single-cooper-pair box. Nature (1999). https://doi.org/10.1038/19718
7. H.. Mooij, Superconducting quantum bits. Phys. World (2004). https://doi.org/10.1088/2058-7058/17/12/30

8. V. Schmidt, Design, fabrication and test of a four superconducting quantum-bit processor (2015). https://theses.hal.science/tel-01214394/document
9. A. Blais, R.-S. Huang, A. Wallraff, S. Girvin, R. Schoelkopf, Cavity quantum electrodynamics for superconducting electrical circuits: an architecture for quantum computation. Phys Rev A (2004). https://doi.org/10.1103/physreva.69.062320
10. A. Wallraff, D. Schuster, A. Blais, S. Girvin, R. Schoelkopf et al., Strong coupling of a single photon to a superconducting qubit using circuit quantum electrodynamics. Nature (2004). https://doi.org/10.1038/nature02851
11. M.H. Devoret, A. Wallraff, J.M. Martinis, Superconducting qubits: a short review, arXiv (2004). https://doi.org/10.48550/arXiv.cond-mat/0411174
12. S. Girvin, M. Devoret, R. Schoelkopf, Circuit QED and engineering charge based superconducting qubits. Phys. Scr. (2009). https://doi.org/10.1088/0031-8949/2009/t137/014012
13. D. Schuster, *Circuit Quantum Electrodynamics* (2007). https://rsl.yale.edu/sites/default/files/files/RSL_Theses/SchusterThesis.pdf
14. Y. Reshitnyk et al., 3D microwave cavity with magnetic flux control and enhanced quality factor. EPJ Quant. Technol. (2016). https://doi.org/10.1140/epjqt/s40507-016-0050-8
15. H. Paik, M. Devoret et al., Observation of high coherence in Josephson junction qubits measured in a three-dimensional circuit QED architecture. Phys. Rev. Lett. (2011). https://doi.org/10.1103/physrevlett.107.240501
16. J. Koch, T.M. Yu, J. Gambetta, A. Houck, D. Schuster, J. Majer, A. Blais, M. Devoret, S. Girvin, R. Schoelkopf, Charge insensitive qubit design derived from the Cooper pair box. Phys. Rev. A (2007). https://doi.org/10.1103/physreva.76.042319
17. N.K. Langford, *Circuit QED–Lecture Notes*, arXiv (2013). https://doi.org/10.48550/arXiv.1310.1897
18. A. Dewes, R. Lauro, F.R. Ong, V. Schmitt, P. Milman, P. Bertet, D. Vion, D. Esteve, Quantum speeding-up of computation demonstrated in a superconducting two-qubit processor. Phys Rev B (2012). https://doi.org/10.1103/PhysRevB.85.140503
19. B.R. Johnson, *Controlling Photons in Superconducting Electrical Circuits* (2011). https://rsl.yale.edu/sites/default/files/files/RSL_Theses/johnson-thesis.pdf
20. A. Houck, J. Gambetta, M. Devoret, R. Schoelkopf et al., Controlling the spontaneous emission of a superconducting transmon qubit. Phys. Rev. Lett. (2008). https://doi.org/10.1103/physrevlett.101.080502
21. E.A. Sete et al., Quantum theory of a bandpass Purcell filter for qubit readout. Phys. Rev. Lett. (2015). https://doi.org/10.1103/physreva.92.012325
22. M. Reagor, H. Paik et al., Reaching 10 ms single photon lifetimes for superconducting aluminum cavities. Appl. Phys. Lett. (2013). https://doi.org/10.1063/1.4807015
23. A. O'Connell, J. Martinis, A. Cleland et al., Quantum ground state and single-phonon control of a mechanical resonator. Nature (2010). https://doi.org/10.1038/nature08967
24. R. Barends, J. Martinis, A. Cleland, Coherent Josephson qubit suitable for scalable quantum integrated circuits. Phys. Rev. Lett. (2013). https://doi.org/10.1103/physrevlett.111.080502
25. J. Rahamim, P. Leek et al., Double-sided coaxial circuit QED with out-of-plane wiring. Appl. Phys. Lett. (2017). https://doi.org/10.1063/1.4984299
26. E. Hyyppä, M. Möttönen, et al. *Unimon qubit*, arXiv (2022). https://doi.org/10.1038/s41467-022-34614-w
27. E. Lucero, J. Martinis et al., Computing prime factors with a Josephson phase qubit quantum processor. Nat. Phys. (2012). https://doi.org/10.1038/nphys2385
28. M. Lyatti, Energy-level quantization and single-photon control of phase slips in YBa2Cu3O7-x nanowires. Nat. Commun. (2020). https://doi.org/10.1038/s41467-020-14548-x
29. F. Bao et al., Fluxonium: an alternative qubit platform for high-fidelity operations. Phys. Rev. Lett. (2022). https://doi.org/10.1103/physrevlett.129.010502
30. L.B. Nguyen, I. Siddiqi et al., Blueprint for a high-performance fluxonium quantum processor. PRX Quant. (2022). https://doi.org/10.1103/prxquantum.3.037001
31. A. Somoroff, V. Manucharyan et al, *Millisecond Coherence in a Superconducting Qubit*, arXiv (2021). arXiv:https://arxiv.org/abs/2103.08578
32. L.B. Nguyen, V.E. Manucharyan, et al. *The High-Coherence Fluxonium Qubit*, arXiv (2018). https://doi.org/10.1103/physrevx.9.041041
33. I.N. Moskalenko, *High Fidelity Two-Qubit Gates on Fluxoniums Using a Tunable Coupler*, arXiv (2022). https://doi.org/10.1038/s41534-022-00644-x
34. E. Hubenschmid, *Transmon and Fluxonium Qubits*, arXiv (2020). https://theorie.physik.uni-konstanz.de/burkard/sites/default/files/images/Seminar_3_TrFl.pdf
35. Y.-H. Lin, L.B. Nguyen, N. Grabon, J.S. Miguel, N. Pankratova, V.E. Manucharyan, Demonstration of protection of a superconducting qubit from energy decay. Phys. Rev. Lett. (2018). https://doi.org/10.1103/PhysRevLett.120.150503
36. L.B. Nguyen, Y.-H. Lin, A. Somoroff, R. Mencia, N. Grabon, V.E. Manucharyan, High-coherence fluxonium qubit. Phys. Rev. Lett. (2018). https://doi.org/10.1103/PhysRevX.9.041041
37. H. Zhang, S. Chakram, T. Roy, N. Earnest, Y. Lu, Z. Huang, D.K. Weiss, J. Koch, D.I. Schuster, Universal fast-flux control of a coherent, low-frequency qubit. Phys. Rev. X (2021). https://doi.org/10.1103/PhysRevX.11.011010
38. J. Koch, J. Gambetta, A. Blais, M. Devoret, R. Schoelkopf et al., Charge insensitive qubit design derived from the Cooper pair box. Phys. Rev. A (2007). https://doi.org/10.1103/physreva.76.042319
39. R. Zhao et al. *Merged-Element Transmon*, arXiv (2020). https://doi.org/10.1103/physrevapplied.14.064006
40. H.J. Mamin et al, *Merged-Element Transmons: Design and Qubit Performance*, arXiv (2021). https://doi.org/10.1103/physrevapplied.16.024023
41. M. Devoret, Implementing qubits with superconducting integrated circuits. Quant. Inf. Process. (2004). https://doi.org/10.1007/s11128-004-3101-5
42. C. Yu, H. Wang, C. Shi, J. Hu, S. Han, R. Wu, R. McDermott, P. Kumar, J. Freeland, D. Pappas, *Flux Noise in Superconducting Qubits* (2015). https://cmsr.rutgers.edu/docman-lister/cmsr/1330-clare-yu/file
43. A. Zazunov et al., Andreev level qubit. Phys. Rev. Lett. (2003). https://doi.org/10.1103/physrevlett.90.087003
44. A. Zazunov et al., Dynamics and phonon-induced decoherence of Andreev level qubit. PRB (2005). https://doi.org/10.1103/physrevb.71.214505
45. C. Janvier, *Coherent Manipulation of Andreev Bound States in an Atomic Contact* (2016). https://doi.org/10.48550/arXiv.1509.03961
46. M. Hays, M. Devoret et al., Coherent manipulation of an Andreev spin qubit. Science (2021). https://doi.org/10.1126/science.abf0345
47. M. Pita-Vidal et al, *Direct Manipulation of a Superconducting Spin Qubit Strongly Coupled to a Transmon Qubit*, arXiv (2022). https://doi.org/10.48550/arXiv.2208.10094
48. V. Fatemi, M.H. Devoret, Going with the grains. Science **372**(6541), 464 (2021). https://doi.org/10.1126/science.abd8556
49. C. Metzger, C. Urbina, H. Pothier et al., *Circuit-QED with Phase-Biased Josephson Weak Links* arXiv (2021). https://doi.org/10.1103/physrevresearch.3.013036
50. A. Joshi et al., Quantum information processing with bosonic qubits in circuit QED. Quant. Sci. Technol. (2021). https://doi.org/10.1088/2058-9565/abe989

51. Y. Wang, *Quantum Error Correction with the GKP Code and Concatenation with Stabilizer Codes*, arXiv (2019). https://doi.org/10.48550/arXiv.1908.00147
52. A. Gyenis, A. Blais, A.A. Hook, D.I. Schuster et al., *Moving Beyond the Transmon: Noise-Protected Superconducting Quantum Circuits*, arXiv (2021). https://doi.org/10.1103/prxquantum.2.030101
53. W.C. Smith, A. Kou, X. Xiao, U. Vool, M.H. Devoret, Superconducting circuit protected by two-Cooper-pair tunneling. NPI Quant. Inf. (2020). https://doi.org/10.1038/s41534-019-0231-2
54. B. Royer, S. Sing, S.M. Girvin, *Encoding Qubits in Multimode Grid States*, arXiv (2022). https://doi.org/10.1103/prxquantum.3.010335
55. M. Zanner et al., Coherent control of a multi-qubit dark state in waveguide quantum electrodynamics. Nat. Phys. (2022). https://doi.org/10.1038/s41567-022-01527-w
56. A. Blais, A. Wallraff et al., *Circuit Quantum Electrodynamics*, arXiv (2020). https://doi.org/10.1103/revmodphys.93.025005
57. P. Krantz et al., A quantum engineeŕs guide to superconducting qubits. Quant. Phys. (2019). https://doi.org/10.1063/1.5089550
58. W.C. Smith et al., Superconducting circuit protected by two-Cooper-pair tunneling. NPJ Quant. Inf. (2020). https://doi.org/10.1038/s41534-019-0231-2
59. H. Mooij, Superconducting quantum bits. Phys. World (2004). https://doi.org/10.1088/2058-7058/17/12/30
60. M. Jerger aus Bahl, *Experiments on Superconducting Qubits Coupled to Resonators* (2013). https://publikationen.bibliothek.kit.edu/1000033614/2479290
61. U. Vool, M. Devoret, *Introduction to Quantum Electromagnetic Circuits*, arXiv (2017). https://doi.org/10.1002/cta.2359
62. J. Yu, E. Solano et al., *Superconducting Circuit Architecture for Digital-Analog Quantum Computing*, arXiv (2022). https://doi.org/10.1140/epjqt/s40507-022-00129-y
63. A. Di Paolo, A. Blais, W.D. Oliver et al., Extensible Circuit-QED Architecture Via amplitude- and frequency-variable microwaves, arXiv (2022). https://doi.org/10.48550/arXiv.2204.08098
64. Y. Sunada, Y. Nakamura et al., *Fast Readout and Reset of a Superconducting Qubit Coupled to a Resonator with an Intrinsic Purcell Filter*, arXiv (2022). https://doi.org/10.1103/physrevapplied.17.044016
65. S. Li, J.-W. Pan et al., Realization of fast all-microwave CZ gates with a tunable coupler. Chin. Phys. Lett. (2022). https://doi.org/10.1088/0256-307x/39/3/030302
66. X. Pan et al., *Engineering Superconducting Qubits to Reduce Quasiparticles and Charge Noise*, arXiv (2022). https://doi.org/10.1038/s41467-022-34727-2
67. J. Larson, T.K. Mavrogordatos, *The Jaynes–Cummings Model and Its Descendants*, arXiv (2022). https://doi.org/10.48550/arXiv.2202.00330
68. G. Xiu et al., Microwave photonics with superconducting quantum circuits. Phys. Rep. (2019). https://doi.org/10.1016/j.physrep.2017.10.002
69. J.J. Burnett et al., Decoherence benchmarking of superconducting qubits. NPJ Quant. Inf. (2019). https://doi.org/10.1038/s41534-019-0168-5
70. P. Krantz et al., *A Quantum Engineer's Guide to Superconducting Qubits*, arXiv (2019). https://doi.org/10.48550/arXiv.1904.06560
71. Y. Xu, I. Siddiqi et al., *Radio Frequency Mixing Modules For Superconducting Qubit Room Temperature Control Systems*, arXiv (2021). https://doi.org/10.1063/5.0055906
72. N. Cottet, *Energy and Information in Fluorescence with Superconducting Circuits* (2018). https://hal.science/tel-02002463/
73. N.P. Breuckmann, J.N. Eberhardt, Quantum low-density parity-check codes. Phys. Rev. X Quant. (2021). https://doi.org/10.1103/PRXQuantum.2.040101
74. J.P.G. van Dijk et al., *The Electronic Interface for Quantum Processors*, arXiv (2019). https://doi.org/10.1016/j.micpro.2019.02.004
75. R. Hicks et al., Active readout-error mitigation. Phys. Rev. A (2021). https://doi.org/10.1103/PhysRevA.105.012419
76. M. Beisel et al., Configurable readout error mitigation in quantum workflows. Electronics (2022). https://doi.org/10.48550/arXiv.2108.12432
77. I. Siddiqi, *Superconducting Circuits Balancing Art and Architecture, QIS Kickoff 2019* (2019). https://www.orau.gov/qispi2018/plenary-talks.htm
78. J. Gambetta et al., Investigating surface loss effects in superconducting transmon qubits. IEEE Trans. Appl. Superconduct. (2017). https://doi.org/10.1109/tasc.2016.2629670
79. I. Holzman, Y. Ivry, On-chip integrable planar nbn nano squid with broad temperature and magnetic-field operation range. AIP Adv. (2019). https://doi.org/10.1063/1.5100259
80. S. Kim et al., *Enhanced Coherence of All-nitride Superconducting Qubits Epitaxially Grown on Silicon Substrate*, arXiv (2021). https://doi.org/10.1038/s43246-021-00204-4
81. J. Zotova et al., *Compact Superconducting Microwave Resonators Based on Al-AlOx-Al Capacitor*, arXiv (2022). https://doi.org/10.48550/arXiv.2203.09592
82. A. Antony et al., *Miniaturizing Transmon Qubits Using van der Waals Materials*, arXiv (2021). https://doi.org/10.21203/rs.3.rs-923599/v1
83. A. Romanenko, R. Pilipenko, S. Zorzetti, D. Frolov, M. Awida, S. Belomestnykh, S. Posen, A. Grassellino, Three-dimensional superconducting resonators at $T<20$ mK with photon lifetimes up to τ=2s, Phys. Rev. A (2020). https://doi.org/10.48550/arXiv.1810.03703
84. A. Grassellino, *Superconducting Quantum Materials and Systems Center*. SQMS Center, Fermilab (2021). https://indico.fnal.gov/event/48767/contributions/212914/attachments/144283/183119/PAC2021SQMS.pdf
85. A. Opremcak, R. McDermott et al., High-fidelity measurement of a superconducting qubit using an on-chip microwave photon counter. Phys. Rev. X (2021). https://doi.org/10.1103/PhysRevX.11.011027
86. Y. Wu, J.-W. Pan et al., Strong quantum computational advantage using a superconducting quantum processor. Phys. Rev. Lett. (2021). https://doi.org/10.1103/PhysRevLett.127.180501
87. Q. Zhu, J.-W. Pan et al., Quantum computational advantage via 60-qubit 24-cycle random circuit sampling. Sci. Bull. (2021). https://doi.org/10.1016/j.scib.2021.10.017
88. J.F. Gonthier, M.D. Radin, C. Buda, E.J. Doskocil, C.M. Abuan, J. Romero, Measurements as a roadblock to near-term practical quantum advantage in chemistry resource analysis. Phys. Rev. Res. (2021). https://doi.org/10.1103/PhysRevResearch.4.033154
89. M. Fellous-Asiani, J.H. Chai, Y. Thonnart, H.K. Ng, R.S. Whitney, A. Auffèves, *Optimizing Resource Efficiencies For Scalable Full-stack Quantum Computers*, arXiv (2022). https://doi.org/10.48550/arXiv.2209.05469
90. A. Auffèves, Quantum technologies need a quantum energy initiative. PRX Quant. (2022). https://doi.org/10.1103/PRXQuantum.3.020101
91. A. Auffèves, O. Ezratty, J. Spletstoesser, R. Whitney, *Quantum Energy Initiative* (2022). https://quantum-energy-initiative.org/